A discussion on the determination of atmospheric OH and its trends

P. Jöckel, C. A. M. Brenninkmeijer, P. J. Crutzen

Atmos. Chem. Phys. Discuss., 2, 1261–1286, 2002
www.atmos-chem-phys.org/acpd/2/1261/

Atmospheric Chemistry and Physics Discussions

A discussion on the determination of atmospheric OH and its trends

P. Jöckel, C. A. M. Brenninkmeijer, and P. J. Crutzen

Max Planck Institute for Chemistry POB 3060, 55020 Mainz, Germany

Received: 17 July 2002 – Accepted: 15 august 2002 – Published: 30 August 2002

Correspondence to: P. Jöckel (joeckel@mpch-mainz.mpg.de)

Abstract

The global hydroxyl radical distribution largely determines the oxidation efficiency of the atmosphere and, together with their sources and atmospheric transport, the distributions and lifetimes of most trace gases. Because of the great importance of several of these gases for climate, ozone budget and OH itself, it is of fundamental importance to acquire knowledge about atmospheric OH and possible trends in its concentrations. In the past, average concentrations of OH and trends were largely derived using industrially produced CH_3CCl_3 as a chemical tracer. The analyses have given valuable, but also rather uncertain results. In this paper we describe an idealized computer aided tracer experiment which has as one of its goals to derive tracer concentration weighted, global average $< k(\mathrm{OH}) >$, where the temporal and spatial OH distribution is prescribed and k is the reaction rate coefficient of OH with a hitherto never produced (Gedanken) tracer, which is injected at a number of surface sites in the atmosphere in well known amounts over a given time period. Using a three-dimensional (3-D) time-dependent chemistry/transport model $< k(\mathrm{OH}) >$ can be accurately determined from the calculated 3-D tracer distribution. It is next explored how well $< k(\mathrm{OH}) >$ can be retrieved solely from tracer measurements at a limited number of surface sites. The results from this analysis are encouraging enough to actually think about the feasibility to carry out a global dedicated tracer experiment to derive $< k(\mathrm{OH}) >$ and its temporal trends. However, before that, we propose to test the methods which are used to derive $< k(\mathrm{OH}) >$, so far largely using CH_3CCl_3, with an idealized tracer experiment, in which a global model is used to calculate the "Gedanken" tracer distribution, representing the real 3-D world, from which we next derive $< k(\mathrm{OH}) >$, using only the tracer information from a limited set of surface sites. We propose here that research groups which are, or will be, involved in global average OH studies to participate in such an inter-comparison of methods, organized and over-seen by a committee appointed by the International Global Atmospheric Chemistry (IGAC) program.

ACPD

2, 1261–1286, 2002

1. Introduction

The primary source of hydroxyl (OH), the atmosphere's "detergent", is photolysis of ozone by solar ultraviolet radiation, $O_3 + h\nu \rightarrow O_2 + O(^1D)$, followed by $O(^1D) + H_2O \rightarrow 2OH$. OH mainly reacts with CH_4 and CO in most of the atmosphere, but does also with almost all other gases that are released into the atmosphere by natural processes and human activities. OH is also substantially recycled, for instance by the reaction $NO + HO_2 \rightarrow OH + NO_2$, thus causing a strong dependence also on highly variable NO_x (= NO + NO_2), which is produced by very discontinuous and quantitatively not well known processes, such as lightning, soil exhalations, and fossil fuel and biomass combustion. All these factors lead to very large spatial and temporal variations, which render it practically impossible to determine global average OH by direct observations. Yet, the global average effect of hydroxyl radicals on trace gas removal and how this may change with time is clearly important to quantify.

The main experimental method to assess global OH was pioneered by Lovelock (1977) and Singh (1977), who measured the industrial chemical CH_3CCl_3 (a solvent, known as methylchloroform, MCF) which was released at approximately known rates into the atmosphere, and which is removed mainly by reaction with OH. Since then, the "MCF method" has been adopted in many studies (Prinn et al., 1983a,b, 1987; Spivakovsky et al., 1990; Hartley and Prinn, 1991; Spivakovsky et al., 1991; Cunnold and Prinn, 1991; Spivakovsky, 1991; Prinn et al., 1992, 1995; Krol et al., 1998), making use especially of the ALE/GAGE/AGAGE (Prinn et al., 1983a,b) and other sampling networks (e.g. NOAA/CMDL (Montzka et al., 2000)). Prinn et al. (2001) used sophisticated statistical tools and a 12-box atmospheric model to derive absolute values and trends in MCF weighted global average OH concentrations. In their most recent study they estimate rather large, but also quite uncertain trends with an increase in global average MCF weighted OH levels by 15±20% between 1979 and 1989, followed by a sharp decline to reach in the year 2000 values even 10±24% below those in 1979. Krol et al. (1998) used an Eulerian three-dimensional (longitude, latitude, pressure),

ACPD
2, 1261–1286, 2002

time dependent chemistry transport model to simulate MCF time series arriving at an upward trend of 6.9±9% from 1978 to 1993, in line with the most recent estimates by Prinn et al. (2001). Maybe not unrelated, the large break in OH trends from 1979–1989 to 1989–2000, derived by Prinn et al. (2001) approximately coincides with a major change in MCF emissions from growth to rapid decline caused by the phase-out of its production. If MCF emissions were underestimated during the most recent period, this could explain the rapid decline in estimated OH.

Currently the MCF inventory of the atmosphere decreases by about 16% per annum, which at the present level of 40 pmol/mol is equivalent to roughly 10^9 kg of this chemical. In the future, CH_3CCl_3 sources from remaining storage, from developing nations, and possibly nature (Rudolph et al., 2000) may become significant for OH retrieval studies. The pertinent question arises, how to better proceed in the future.

Because MCF is banned for its ozone depleting properties, it is not useful, even when levels have further decreased, to contemplate future releases for the sole purpose of its continued use as a tracer. Nevertheless, there are already some potential alternatives in the atmosphere. The compounds which replace the CFCs (chlorofluoro carbon), the HCFCs (hydrogen chlorofluoro carbon) and HFCs (hydrofluoro carbons), react with OH and can serve as chemical trace gases to estimate "global average OH". Inspection of the worldwide production data (http://www.afeas.org) shows, however, strong changes, lessening their suitability as tracers. (For instance, HFC134a production increased from 1998 to 1999 more than sixfold to a total of 133662 metric tons; its concentration is now in the lower pmol/mol range). Nevertheless with the inventory increasing, and production leveling off, relative growth rates decline, so that with a lifetime of the order of 14 years HFC134a and other HFCs may become promising replacements for MCF as chemical tracers. A requirement for its suitability, to serve as a global average OH probe, is accurate reporting of times and locations of release. It is questionable whether this criterion can be satisfied.

Because of the fundamental importance of OH as the atmosphere's cleansing agent we should consider the use of a new dedicated tracer, without any natural or anthro-

pogenic sources, to estimate "global average OH" and its trends, or to test the methods which have been applied so far to obtain that quantity.

2. An ideal tracer experiment

We here explore properties and limitations of the tracer method. Ideally, measurement of a tracer at a sufficient number of sites should allow determination of characteristics of global OH. Is this feasible? To answer this question, we performed ideal tracer model simulations – Computer Aided Gedanken Experiments (CAGEs), using a 3-D Chemistry Transport Model (CTM) (see Appendix A: Model setup). A new MCF-like tracer with a perfectly known rate coefficient for reaction with OH ($k_{OH} = 1.8 \cdot 10^{-12} \cdot e^{\frac{-1555\,K}{T}}$), being its only sink, is supposed to be released continuously in known quantities at the surface during January 1993 at 9 sites listed in Table 1 (see Appendix A: Model setup). (We note that sensitivity studies with different release points (results not shown) showed that the results are virtually independent from the starting conditions.) From there the tracer spreads throughout the atmosphere whilst reacting with a prescribed OH distribution featuring the typical strong maximum in the tropics where solar ultraviolet radiation, temperatures and water vapor concentrations peak. Monthly varying mean OH concentrations for the troposphere were taken from Spivakovsky et al. (2000) and combined with monthly mean stratospheric OH distributions calculated with a 2-D model (C. Brühl, unpublished results, personal communication, 2002). The resulting global distribution was repeatedly prescribed for all years during the entire numerical tracer experiment period which lasted from the beginning of 1993 to the end of 1997. The meteorological fields (winds, temperatures, cloudiness, convection, sub-grid diffusion, etc.) varied, however, inter-annually. We use the CTM to generate pseudo-tracer distributions. From these we calculate the global tracer mass as integral over the model atmosphere. The time dependence of the global tracer mass determines the tracer lifetime. Thereafter we try to reconstruct this "true" tracer lifetime, using only tracer time series sampled from the pseudo tracer distribution at a selected sampling network, for

ACPD
2, 1261–1286, 2002

example at the 5 stations of the ALE/GAGE/AGAGE network (see Table 2, Appendix A: Model setup).

The (e-folding) lifetime τ (exponential decay, or "turnover" time), or its inverse, globally averaged, tracer concentration weighted, $< k(\mathrm{OH}) >$ is defined by

$$\tau(t) := -\frac{M(t)}{dM/dt} = \frac{\int \mu \rho dV}{\int k(\mathrm{OH}) \mu \rho dV} =: 1/ < k(\mathrm{OH}) > \quad (1)$$

with $M(t)$ the tracer mass at time t, k the reaction rate coefficient, (OH) the OH concentration per unit volume, μ the tracer mass mixing ratio, and ρdV the atmospheric mass differential. An important point to note is that $1/\tau$, does not give global average ($\bar{\mathrm{OH}}$), but $< k(\mathrm{OH}) >$, that is (OH) weighted by temperature dependent k and the tracer mixing ratio, integrated over the mass of the atmosphere (for a derivation see Appendix B: Global average tracer lifetime).

Because of the dependence on tracer distribution, inter-annual changes in meteorology affect $< k(\mathrm{OH}) >$. To indicate its significance we show in Fig. 1a, using the full tracer model information, the ratios of calculated lifetimes τ (Eq. (1), left) for the year 1995 and 1997 compared to 1996. We note changes in the order of about 1%, despite the fact that OH concentrations did not change between the years. This shows that "global average OH" is not a satisfactory quantity to define the oxidizing power of the atmosphere. The effect of meteorology is caused by changes in the distributions of temperature and tracer. As also mentioned by Lawrence et al. (2001), the more rapid the transport of the tracer to the high temperature – high OH regions of the tropics, the shorter the tracer lifetime. This implies that separation of changes of $< k(\mathrm{OH}) >$ into dynamical and chemical causes is problematic. It means that, even for the ideal tracer case, variations in OH from year to year, except if they are unrealistically large (of the order of 1%/a or more), cannot be detected. We also note that $< k(\mathrm{OH}) >$ derived for one tracer cannot be strictly used to derive $< k(\mathrm{OH}) >$ for another tracer by simple temperature adjustment of the reaction rate coefficient, applying a global average temperature of 277 K (Prather and Spivakovsky, 1990). This is only possible if

(a) the temperature dependencies of their reaction coefficients are similar, and

(b) their distributions and locations of sources and sinks are approximately the same.

So far, our analysis used full 3-D model information about relative changes in tracer mass, $M(t)$ with time. In practice, such information must be estimated from the limited set of surface observations if no additional model information is used, which could make the results dependent on the veracity of the model. In the following, using the simplest possible approach, we will see how far we can get only using the limited tracer information.

Relative changes in tracer mass, $M(t)$, with time and the tracer lifetime τ may be obtained from the global average mixing ratio ($\tilde{\mu}$), which may be approximated from the values at the measurement sites (s) at latitudes Φ_s

$$\tilde{\mu} \approx \frac{\sum_s \mu_s w(\Phi_s)}{\sum_s w(\Phi_s)} ; \tilde{\tau} = -\frac{\tilde{\mu}}{d\tilde{\mu}/dt} \quad (2)$$

where w is an appropriate weighting function, e.g. $w_1(\Phi) = cos(\Phi)$, or $w_2 = 0.5(cos(\Phi + \Delta_1\Phi) - cos(\Phi - \Delta_2\Phi))$ with $\Delta_1\Phi$ and $\Delta_2\Phi$ being the latitudes differences halfway to bordering stations with adjustments towards the poles. In this case we neglect the effect of vertical gradients in $\tilde{\mu}$ and μ_s.

Figure 2 shows the calculated average tracer lifetime τ, derived from Eq. (1, left) with the full tracer information, and from Eq. (2) from samples of μ_s at the indicated stations. For the stations we may for instance choose the ALE/GAGE/AGAGE sites, (cases a and b), or 100 randomly chosen stations (case c). For case b we assumed that we have access to vertical column information which could in principle be obtained from optical instruments, thus replacing μ_s in Eq. (2) by the vertically, air mass weighted average mixing ratio. $\tilde{\mu}$ (Eq. (2)) was calculated with w_2 for cases a and b, and with w_1 for case c. The result has been smoothed over 60 days (i.e. 12 model output time steps) to reduce much of the scatter caused by variable meteorology. Most of the sinusoidal variation results from a slight NH/SH asymmetry, with more OH in the adopted data

set of Spivakovsky et al. (2000) in the NH (which may be unrealistic). Note that the increased variability in Jan/Feb 1996 (cf. the peak in Fig. 2a) can only be traced back to local artifacts in the underlying meteorological data of the model experiment.

The actual lifetimes in years (see numbers in Fig. 2) and standard deviations for 1995, 1996 and 1997 are derived from the full information (left) and from the reduced (stations only) information (right) as

$$\bar{\tau} = \frac{\sum_{i=1}^{N} \tau(t_i)}{N} ; \sigma_{\bar{\tau}} = \left(\frac{\sum_{i=1}^{N} (\tau(t_i) - \bar{\tau})^2}{N}\right)^{\frac{1}{2}} , \quad (3)$$

where $N = 73$ is the number of (5-day averaged) model output time steps per year.

We calculate intra-annual variabilities in inferred tracer lifetimes of ±7% in the former and up to ±17%, including uncertainties, in the latter case. Annual mean tracer lifetimes derived from the limited sampling network deviate by about 2% from those derived with the full information. If vertical column tracer information were available, annual mean tracer lifetimes would be within 0.3% at best of the full information values (Fig. 2b).

Using only the (limited) station observation also leads to large uncertainties in the monthly averaged lifetimes. In Fig. 1b we show the relative differences in lifetimes (monthly averages) for the MCF type tracer for the years 1995 and 1997 compared to 1996 for the AGAGE stations case. The high variations of the order of up to ±20%, even after 60-day smoothing, compared to only about 1% for the full model, is due to inter-annual differences in meteorology and lack of information about the tracer distribution. The situation can be improved if vertically integrated tracer information (as might be obtained using optical techniques) is used. As shown in Fig. 1c for the 5 stations, the inter-annual variability can be significantly reduced (by about ±5%). The foregoing shows that the limited information from the station network causes considerable problems in deriving relative changes in tracer mass over the whole atmosphere. It should be mentioned that approximating the column information by an additional weighting (Eq. (2)) by $w_3 = (p_s - p_{tp})/p_s$, (with p_s being the surface pressure, and

ACPD
2, 1261–1286, 2002

p_{tp} the tropopause pressure), neglecting the amount of tracer in the stratosphere did not improve the results, because it did not reduce the variability of the averaged tracer mixing ratio ($\tilde{\mu}$ in Eq. (2)).

We also performed simulations using sets of tracer pairs with mutually slightly different rate coefficients with OH, in the hope of obtaining more stable $< k(\mathrm{OH}) >$ results by eliminating part of the variability due to meteorology. Also this attempt did not improve the results.

In summary, the results indicate that using the total tracer column information at a given set of sampling locations could substantially improve the results, i.e. leading to lower uncertainties, compared to using only the surface information which neglects vertical gradients. It is unlikely, however, if the detection limit of optical techniques can be made low enough to be applicable to a realistic amount of released tracer mass, which can be excluded for a dedicated tracer. It should be explored, however, if any industrial tracers already in production, in particular the HCFCs of HFCs, may be suitable candidates for total column determination.

3. Optimizing the sampling strategy

We have arbitrarily used the AGAGE network as a choice of sampling locations. The question arises whether, and if so, how, uncertainties can be reduced by optimizing the locations of sampling sites. The results for 100 randomly chosen locations (Fig. 2c) indicate that with an increased number of measurement sites the uncertainties decrease.This decrease with an increasing number of stations is, however, very slow (not shown). Furthermore, operating a large number of sampling sites over a long time period is not practical.

Facing these limitations, we next discuss possible criteria for finding an "optimized sampling strategy", in order to minimize the uncertainties based on surface observations. Since the crucial problem is tracer variability, one strategy could be trying to minimize the signal to noise ratio, i.e. to search sampling sites with a minimal rela-

ACPD
2, 1261–1286, 2002

tive variability σ_μ/μ (where σ is the standard deviation over a time interval). However, evidently, the spatial distribution of this ratio depends on the time scale as shown in Fig. 3.

The 1 year variability (lower panel) is determined by the local seasonal cycle of OH. For instance, the prescribed OH distribution shows a larger seasonal OH amplitude in the NH compared to the SH. A naive choice of "optimal" sampling locations would only cover the SH, and not be representative for the whole globe. In contrast, the (annually averaged) relative short time (here 5-day) variability gives information about the meteorological variations (since OH is monthly averaged). This pattern (upper panel) probably depends on the used model and/or on the quality of the driving meteorological data (for CTMs).

A second strategy, focusing more on the "representativeness" of the potential locations, can be devised by comparing the "local lifetime" $\tau_s = -\mu_s/(d\mu_s/dt)$ (cf. Eq. (1), left) with the global average lifetime derived from the global tracer mass (Eq. (1), left). A three-year (1995–1997) average ratio of those lifetimes is shown in Fig. 4. The figure (upper panel) shows a rather complex distribution of this ratio, which is, e.g. due to the atmospheric transport, not directly correlated with the local annual average OH concentration. Therefore, also the locations found by this strategy (minimum of the ratio, see lower panel) are dependent on the OH distribution, the model, and the underlying meteorology.

A third alternative strategy for a systematic choice of sampling locations, is a combination of the two previously discussed. Whereas the first strategy only focuses on the tracer variability, and the second strategy only on the average lifetime, minimizing the average (ΔT) RMS-deviation between "local" (τ_s) and global lifetime (τ) identifies those sites, where on average, the global lifetime is captured by the local lifetime, but additionally with smallest possible differences:

$$RMS = \left(\frac{\sum(\tau_s(t) - \tau(t))^2}{\Delta T}\right)^{\frac{1}{2}} \quad (4)$$

The three-year averaged RMS deviation is shown in Fig. 5. The result (upper panel)

looks similar to that of strategy 2. Also here, the distribution of the resulting "optimal" locations (lower panel) cannot be easily explained.

We summarize that the outcome of all 3 strategies is more or less dependent on the model, the meteorological data, and the OH distribution. And especially for the latter we end up with a circular problem, because the aim was to derive information about global OH. Nevertheless, we could apply the results and sample in a self consistent way at the locations defined by the various strategies, in order to see whether the uncertainties (i.e. the standard deviation in Fig. 2) become smaller and therefore closer to the "annual standard deviation" (derived from full global information). Surprisingly, this was not the case (results not shown). A possible explanation, however, arises from the degree of correlation between the different locations: All three strategies above treat every location (model grid cell) as independent and suggest those, where the applied criteria is "optimal". One single "optimal" location, however, is evidently not enough to derive the global quantity τ, and the uncertainty is very large. Therefore, the information from a number of stations is combined (Eq. (2)). If the tracer mixing ratio time series at these locations are well correlated w.r.t. their variation around the average, the uncertainty caused by the variability will not cancel out as it would for a set of completely de-correlated ("white noise") locations. The most important criterion for an optimal set of sampling locations is therefore a minimum correlation between them. This, however, is difficult to derive systematically.

4. Potential tracers

Given the importance of OH, as reiterated in countless publications, one wonders whether reliance on "accidental tracers", i.e. emission of chemicals that react with OH, is wise. The global atmosphere comprises $1.77 \cdot 10^{20}$ mol air, and low detection limits are required for executing a real tracer experiment. The lowest detection limits reached to date are for ^{14}CO. This molecule, of which 13–16 kg is produced per annum by cosmic radiation can be detected with a ≈1% precision at a concentra-

ACPD
2, 1261–1286, 2002

tion of only 10 molecules per cm^3 air at standard temperature and pressure (approximately $4 \cdot 10^{-7}$ pmol/mol) (Brenninkmeijer, 1993), but ^{14}CO, and radioactive tracers in general are not suited for large scale experiments. However, as we have seen, releases of a host of halocarbons produced by industry appear to be of such a magnitude that they can be detected with good precision, and even the aneastatic Halothane ($CF_3CHBrCl$) is still detectable in the atmosphere (present day mixing ratio around $0.005 \cdot 10^{-12}$ mol/mol, W. J. Sturges, personal communication, 2002) and in air extracted from firn deposits in the polar regions. Thus a global scale controlled experiment entailing the release of a tracer exclusively for better gauging OH, is a matter of cost indeed. The first question then is how cost can be reduced by using the ultimate analytical sensitivity thus reducing the amount of tracer that is required.

Using gas-chromatography mass-spectrometry, detection levels of 10^{-15} have been reached (Sturges et al., 2000). This is based on the preconcentration of condensable trace gases from about 1 l of air followed by gas chromatographic separation and mass spectrometric identification and detection. By scaling up the preconcentration, lower detection limits can be attained, provided certain conditions are met. Assuming for argument sake that a measurement precision of 1% can be reached at 10^{-15} when the preconcentration is based on 100 l of air, $\sim 0.18\, M_{mol}$ ton of tracer substance is required for a global experiment (M_{mol} is the molecular weight of the tracer substance, and no allowance has been made for the decay of the tracer). Through preconcentration at the respective measurement sites by means of absorption tubes, time integration and higher degrees of preconcentration are obtainable.

As to the actual compound that may be suitable we point out that we need a substance with virtually no background level in the atmosphere, that is non-toxic, and that is removed with a suitable lifetime by mainly OH. Deuterated halocarbons form a promising class of compounds. Deuteration at one or more positions is a means of assuring that the background of the substance selected is virtually absent. Second, deuteration can be used to taylor the reaction rate constant of the compound to give a suitable lifetime. Third, deuteration is a cheap way of labeling.

It is beyond the scope of this paper to elaborate on concrete tracers, and the total cost of such a program, which after all involves, the production, release, sampling and analyses, but we point out that it may well be that the production cost of the tracer substance is moderate in comparison to the cost of the sampling and analysis.

5. Conclusions

Summarizing, we recall that past derivations of "global average OH", based on the MCF tracer method have produced rather uncertain results. Facing the great importance to know better the self-cleansing power of the atmosphere and its trend, we therefore proposed to explore the feasibility to conduct an idealized tracer experiment in which a known quantity of tracer is injected over a given period and thereafter measured at a number of sites. To prepare for a real experiment, here first a "Computer Aided Gedanken Experiment" has been conducted. The results are rather encouraging. On an annual average basis, the 5 station information produced annually mean tracer lifetimes within 2% of those which are derived with the full tracer information of the 3-D model, even using no refined inverse analysis. Our estimate does, however, not consider any measurement errors. Judicious choice of the locations of the measurement sites may improve the situation, but such an optimization is also model dependent (the attempts which we tried failed). An "optimized sampling strategy" has to take into account the correlation between the sampling sites in question.

We have shown that, even adopting the same OH fields from year to year, different inter-annual global average tracer lifetimes by about 0.6% are calculated with the full tracer information (see numbers in Fig. 2, left). This is due to varying correlations between tracer mixing ratios, OH concentrations, and temperatures. We note that "global average OH" is not a well suited property to define the oxidizing power of the atmosphere. Further, knowledge of relative changes in $< k(\mathrm{OH}) >$ for one tracer can only be extrapolated without problem to others, when the temperature dependence of the rate coefficients, and spatial and temporal source distributions are similar.

ACPD
2, 1261–1286, 2002

MCF has so far been the best tracer that was available to the atmospheric chemistry community for OH trend analyses (^{14}CO has been available all the time, but regrettably little used); but its concentrations are declining by 16% per year, so that even small residual emissions of MCF can become problematic. Thus we may contemplate other tracers, including dedicated ones (e.g. certain deuterated halocarbons), solely produced and released for estimating their $< k(OH) >$, as simulated in this study by our idealized numerical tracer experiment.

The main intention of this paper is solely to provide an impulse for a further discussion about the feasibility of such an experiment, which has to be carried out at a reasonable cost and supported by a broad community.

6. Proposal

Before a real global tracer experiment should be considered, we propose as a first step to start with an objective inter-comparison of the methods applied so far (and by newcomers) to derive $< k(OH) >$ on the basis of idealized numerical tracer experiments, along the lines shown in this study. The analysis methods could be applied to the same model generated station "pseudo-observations" to see how well it is possible to retrieve $< k(OH) >$ obtained with the full model from the pseudo-observations at the limited number of surface sites. This will provide benchmark tests for the methods which are used by different groups to estimate $< k(OH) >$ and its trends.

Appendix A: Model setup

A tracer with an atmospheric lifetime of approximately 5 years, resembling MCF was assumed to have been injected at the locations listed in Table 1 during January 1993. The global OH distribution and seasonality is prescribed as monthly averages using the results of Spivakovsky et al. (2000) for the troposphere, and the two-dimensional

ACPD
2, 1261–1286, 2002

model results of Ch. Brühl (personal communication, 2002) in the stratosphere, i.e. above the $(300 - 215 * cos^2(\Phi))$ hPa height level. The tracer distributions are integrated with the 3-D model MATCH ("Model of atmospheric chemistry and transport", Rasch et al. (1997)) in the National Center of Atmospheric Research (NCAR) Version 4.0-beta2-1 (http://www.cgd.ucar.edu/cms/match/). The Eulerian grid space comprises 32 latitudes, 64 longitudes, and 28 levels up to approximately 2 hPa. The model is driven by the NCEP-reanalysis data of the years 1993 to 1997 (Kalnay et al., 1996). The tracer advection algorithm is the SPITFIRE (Split implementation of transport using flux integral representation) advection scheme (Rasch and Lawrence, 1998), which is a mass flux form advection scheme. In the current version it comprises a pressure adjustment, in order to avoid tracer mass inconsistencies as reported by Jöckel et al. (2001). Vertical diffusion is parameterized according to Holtslag and Boville (1993). The moist convection is calculated by a combination of the two individual schemes of Zhang and McFarlane (1995) and Hack (1994). The results of the 5 year integration are archived as 5-day averages.

The ALE/GAGE/AGAGE stations have been used as exemplary sampling sites, as listed in Table 2

Appendix B: Global average tracer lifetime

Usage of the terms "global lifetime" and/or "global average OH", require implicitly the assumption of the atmosphere being a single "box", in which OH, temperature T, and the tracer (mass mixing ratio μ) are homogeneously distributed.

Within such a box the change of tracer concentration C with time t is determined by a first order reaction with OH

$$\frac{dC}{dt} = -k(T) \cdot [\mathrm{OH}] \cdot C + e(t), \tag{5}$$

where $e(t)$ is the source strength and k the reaction coefficient. Multiplying by $\frac{V \cdot m_m^t}{N_a}$,

with V being the (constant) box volume, m_m^t the molar mass of the tracer, and N_a the Avogadro constant, Eq. (5) also holds for the tracer mass

$$\frac{dM}{dt} = -k(T) \cdot [\mathrm{OH}] \cdot M + \tilde{e}(t). \tag{6}$$

In the experiment described above, $e(t > t_0) = 0$. In this case the "lifetime" of the tracer is well defined

$$\tau = \frac{1}{k(T) \cdot [\mathrm{OH}]} \tag{7}$$

and [OH] is evidently the average.

For an equivalent derivation for the global atmosphere, the change with time of the tracer concentration in a volume element dV is (e taken here to be zero !)

$$\frac{dC(\boldsymbol{r}, t)}{dt} = -k(T(\boldsymbol{r}, t)) \cdot [\mathrm{OH}](\boldsymbol{r}, t) \cdot C(\boldsymbol{r}, t) + f(\boldsymbol{r}, t). \tag{8}$$

$\boldsymbol{r}$ is the 3-dimensional vector in space, and f the net flux of tracer from/to neighboring volume elements.

Since the tracer concentration can be expressed in terms of the mass mixing ratio μ and the air density ρ

$$C(\boldsymbol{r}, t) = \rho(\boldsymbol{r}, t)\mu(\boldsymbol{r}, t)\frac{N_a}{m_m^t}, \tag{9}$$

Eq. (8) becomes

$$\frac{d(\mu\rho)}{dt} = -k[\mathrm{OH}]\mu\rho + f\frac{m_m^t}{N_a}. \tag{10}$$

Integration over the total volume of the atmosphere yields after changing the order of integration and time derivative on the left hand side the change with time of the global tracer mass

$$\frac{dM}{dt} = -\int k[\mathrm{OH}]\mu\rho dV \tag{11}$$

with

$$M = \int \mu \rho dV. \tag{12}$$

The global integral over the net flux f vanishes.

The terms under the integral on the right hand side of Eq. (11) depend all on $\boldsymbol{r}$ and t. Therefore the change of tracer mass with time

$$\frac{dM}{dt} \neq -\bar{k} \cdot [\bar{OH}] \cdot M \tag{13}$$

with $\bar{k}$ and $[\bar{OH}]$ being the global air mass weighted averages, in contrast to the simple box case above (Eq. (6)).

References

Brenninkmeijer, C. A. M.: Measurement of the abundance of ^{14}CO in the atmosphere and the $^{13}C/^{12}C$ and $^{18}O/^{16}O$ ratio of atmospheric CO with applications in New Zealand and Antarctica, J. Geophys. Res., 98, 10 595–10 614, 1993. 1272

Cunnold, D. M. and Prinn, R. G.: Comment on "Tropospheric OH in a three-dimensional chemical tracer model: An assessment based on observations of CH_3CCl_3" by C. M. Spivakovsky et al., J. Geophys. Res., 96, 17 391–17 393, 1991. 1263

Hack, J. J.: Parameterization of the moist convection in the national center for atmospheric research community climate model (CCM2), J. Geophys. Res., 99, 5551–5568, 1994. 1275

Hartley, D. and Prinn, R.: Comment on "Tropospheric OH in a three-dimensional chemical tracer model: An assessment based on observations of CH_3CCl_3" by C. M. Spivakovsky et al., J. Geophys. Res., 96, 17 383–17 387, 1991. 1263

Holtslag, A. A. M. and Boville, B. A.: Local versus nonlocal boundary-layer diffusion in a global climate model, J. Climate, 6, 1825–1842, 1993. 1275

Jöckel, P., von Kuhlmann, R., Lawrence, M. G., Steil, B., Brenninkmeijer, C. A. M., Crutzen, P. J., Rasch, P. J., and Eaton, B.: On a fundamental problem in implementing flux-form advection schemes for tracer transport in 3-dimensional general circulation and chemistry transport models, Q. J. R. Meteorol. Soc., 127, 1035–1052, 2001. 1275

Kalnay, E., Kanamitsu, M., Kistler, R., Collins, W., Deaven, D., Gandin, L., Iredell, M., Saha, S., White, G., Woollen, J., Zhu, Y., Chelliah, M., Ebisuzaki, W., Higgins, W., Janowiak, J., Mo, K. C., Ropelewski, C., Wang, J., Leetmaa, A., Reynolds, R., Jenne, R., and Joseph, D.: The NCEP/NCAR 40-year reanalysis project, Bul. Am. Met. Soc., 77, 437–471, 1996. 1275

Krol, M., van Leeuwen, P. J., and Lelieveld, J.: Global OH trend inferred from methylchloroform measurements, J. Geophys. Res., 103, 10 697–10 711, 1998. 1263

Lawrence, M. G., Jöckel, P., and von Kuhlmann, R.: What does the global mean OH concentration tell us?, Atmos. Chem. Phys. Discuss., 1, 43–75, 2001. 1266

Lovelock, J. E.: Methyl chloroform in the troposphere as indicator of OH radical abundance, Nature, 267, 32, 1977. 1263

Montzka, S. A., Spivakovsky, C. M., Butler, J. H., Elkins, J. W., Lock, L. T., and Mondeel, D. J.: New observational constraints for atmospheric hydroxyl on global and hemispheric scales, Science, 288, 500–503, 2000. 1263

Prather, M. and Spivakovsky, C. M.: Tropospheric OH and the lifetimes of hydrochlorofluorocarbons, J. Geophys. Res., 95, 18 723–18 729, 1990. 1266

Prinn, R., Cunnold, D., Rasmussen, R., Simmonds, P., Alyea, F., Crawford, A., Fraser, P., and Rosen, R.: Atmospheric trends in methylchloroform and the global average for hydroxyl radical, Science, 238, 945–950, 1987. 1263

Prinn, R., Cunnold, D., Simmonds, P., Alyea, F., Boldi, R., Crawford, A., Fraser, P., Gutzler, D., Hartley, D., Rosen, R., and Rasmussen, R.: Global average concentration and trend for hydroxyl radicals deduced from ALE/GAGE trichloroethane (methyl chloroform) data 1978–1990, J. Geophys. Res., 97, 2445–2461, 1992. 1263

Prinn, R. G., Rasmussen, R. A., Simmonds, P. G., Alyea, F. N., Cunnold, D. M., Lane, B. C., Cardelino, C. A., and Crawford, A. J.: The atmospheric lifetime experiment 5. results for CH_3CCl_3 based on three years of data, J. Geophys. Res., 88, 8415–8426, 1983a. 1263

Prinn, R. G., Simmonds, P. G., Rasmussen, R. A., Rosen, R. D., Alyea, F. N., Cardelino, C. A., Crawford, A. J., Cunnold, D. M., Fraser, P. J., and Lovelock, J. E.: The atmospheric lifetime experiment 1. introduction, instrumentation, and overview, J. Geophys. Res., 88, 8353–8367, 1983b. 1263

Prinn, R. G., Weiss, R. F., Miller, B. R., Huang, J., Alyea, F. N., Cunnold, D. M., Fraser, P. J., Hartley, D. E., and Simmonds, P. G.: Atmospheric trends and lifetime of CH_3CCl_3 and global OH concentrations, Science, 269, 187–192, 1995. 1263

Prinn, R. G., Huang, J., Weiss, R. F., Cunnold, D. M., Fraser, P. J., Simmonds, P. G., McCulloch,

A., Harth, C., Salameh, P., O'Doherty, S., Wang, R. H. J., Porter, L., and Miller, B. R.: Evidence for substantial variations of atmospheric hydroxyl radicals in the past two decades, Science, 292, 1882–1888, 2001. 1263, 1264

Rasch, P. J. and Lawrence, M. G.: Recent developments in transport methods at NCAR, in: B. Machenhauer (Ed.): MPI-Hamburg Report No. 265, 65–75, MPI-Hamburg, 1998. 1275

Rasch, P. J., Mahowald, N. M., and Eaton, B. E.: Representations of transport, convection, and the hydrologic cycle in chemical transport models: Implications for the modeling of short-lived and soluble species, J. Geophys. Res., 102, 28 127–28 138, 1997. 1275

Rudolph, J., von Czapiewski, K., and Koppmann, R.: Emissions of methyl chloroform (CH_3CCl_3) from biomass burning and the tropospheric methyl chloroform budget, 27, 1887–1890, 2000. 1264

Singh, H. B.: Atmospheric halocarbons: Evidence in favour of reduced average hydroxyl radical concentration in the troposphere, Geophys. Res. Lett., 4, 101–104, 1977. 1263

Spivakovsky, C. M.: Reply on comment on "Tropospheric OH in a three-dimensional chemical tracer model: An assessment based on observations of CH_3CCl_3" by C. M. Spivakovsky et al., J. Geophys. Res., 96, 17 395–17 398, 1991. 1263

Spivakovsky, C. M., Yevich, R., Logan, J. A., Wofsy, S. C., McElroy, M. B., and Prather, M. J.: Tropospheric OH in a three-dimensional chemical tracer model: An assessment based on observations of CH_3CCl_3, J. Geophys. Res., 95, 18 441–18 471, 1990. 1263

Spivakovsky, C. M., Yevich, R., Logan, J. A., Wofsy, S. C., McElroy, M. B., and Prather, M. J., Reply on comment on "Tropospheric OH in a three-dimensional chemical tracer model: An assessment based on observations of CH_3CCl_3" by C. M. Spivakovsky et al., J. Geophys. Res., 96, 17 389–17 390, 1991. 1263

Spivakovsky, C. M., Logan, J. A., Montzka, S. A., Balkanski, Y. J., Foreman-Fowler, M., Jones, D. B. A., Horowitz, L. W., Fusco, A. C., Brenninkmeijer, C. A. M., Prather, M. J., Wofsy, S. C., and McElroy, M. B.: Three-dimensional climatological distribution of tropospheric OH: Update and evaluation, J. Geophys. Res., 105, 8931–8980, 2000. 1265, 1268, 1274

Sturges, W. T., Wallington, T. J., Hurley, M. D., Shine, K. P., Sihra, K., Engel, A., Oram, D. E., Penkett, S. A., Mulvaney, R., and Brenninkmeijer, C. A. M.: A potent greenhouse gas identified in the atmosphere: SF_5CF_3, Science, 289, 611–613, 2000. 1272

Zhang, G. J. and McFarlane, N. A.: Sensitivity of climate simulations to the parameterization of cumulus convection in the Canadian Climate Center general circulation model, Atmos. Ocean, 33, 407–446, 1995. 1275

Table 1. Release stations with geographical coordinates and released tracer masses. The tracer masses have been chosen such that in each latitude band the same tracer mass per unit surface is released

Location	Latitude [°N]	Longitude [°E]	Mass [kg]
Ny Ålesund	78.90	11.88	0.0978E+03
Mainz	50.00	8.27	0.2415E+03
San Diego	32.72	-117.16	0.3089E+03
Trivandrum	8.48	76.92	0.2163E+03
Puerto Baquerizo Moreno	-0.90	-89.60	0.2519E+03
Darwin	-12.47	130.83	0.2450E+03
La Serena	-29.91	-71.25	0.3016E+03
Punta Arenas	-53.15	-70.92	0.2457E+03
McMurdo	-77.50	162.00	0.0913E+03

Table 2. The ALE/GAGE/AGAGE sampling sites as used in this study

Location	Latitude [°N]	Longitude [°E]
Ireland	53.0	-10.0
Oregon	45.0	-124.0
Barbados	13.0	-59.0
Samoa	-14.0	171.0
Tasmania	-41.0	145.0

ACPD
2, 1261–1286, 2002

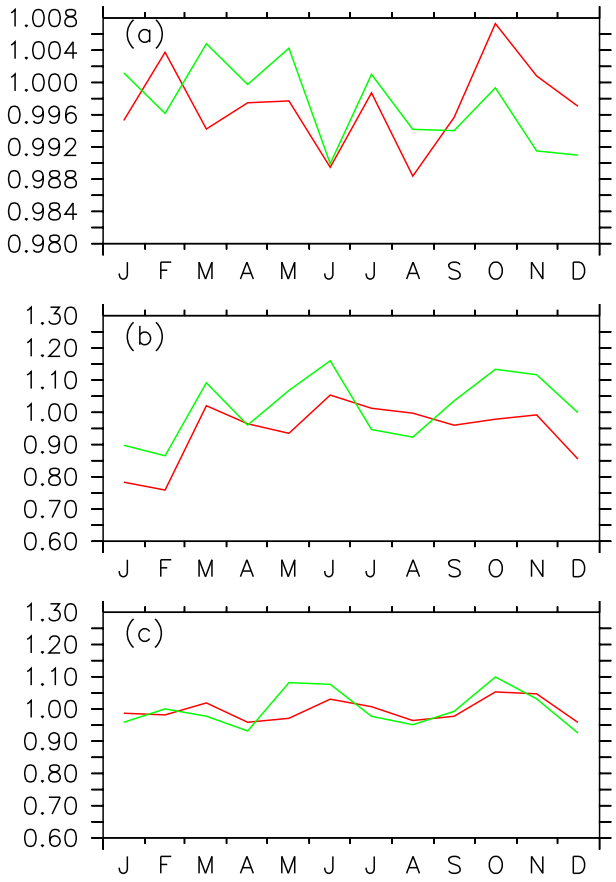

Fig. 1. Inter-annual variation of derived monthly mean lifetime τ for the years 1995 (red) and 1997 (green) for the MCF-like tracer relative to the year 1996, based on full 3-D model information **(a)**, the 5-station surface information (AGAGE) **(b)**, and 5-station total tracer column information **(c)**. Note that the OH concentration distributions were the same for all years.

ACPD

2, 1261–1286, 2002

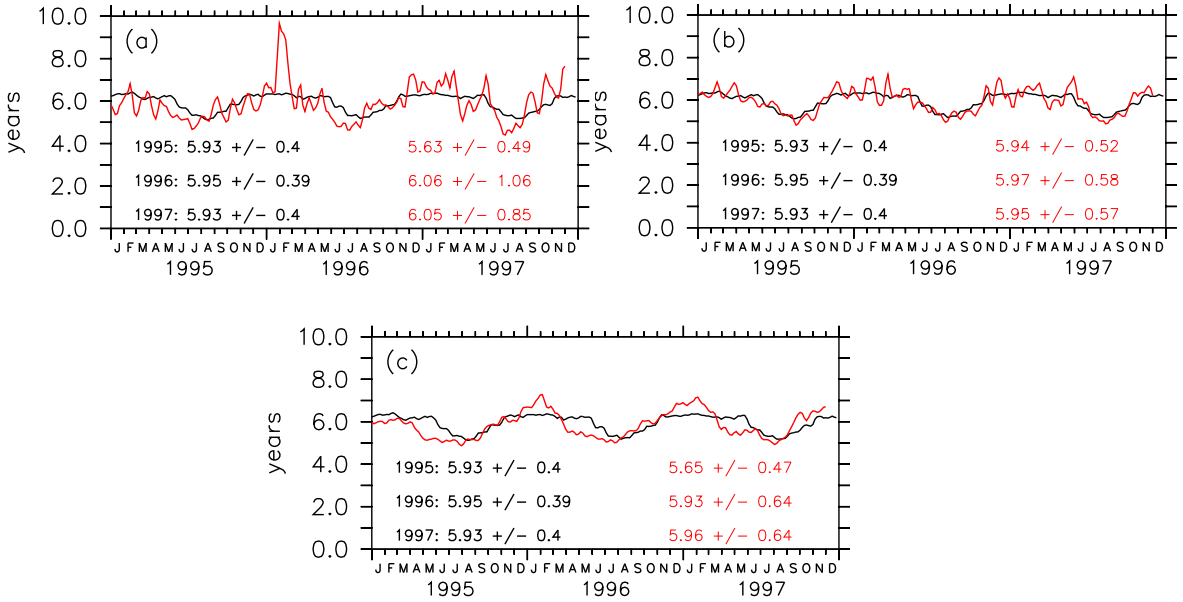

Fig. 2. Estimated global average lifetime (in years) based on the full model information (black, Eq. (1)), and on the tracer information from a set of sampling stations (red, Eq. (2)). Panel **(a)** shows the result using the tracer mixing ratios at the 5 AGAGE stations' surface, in **(b)** the total tracer column information at the 5 AGAGE stations is used, and in (c) the surface information from 100 randomly chosen sampling locations, equally distributed around the globe has been used. The numbers list the annual average lifetime (in years ± standard deviation) derived from the full information (left), and derived from the sampled information (right) for the years 1995, 1996 and 1997. The averaged mass mixing ratio from the station data (Eq. (2)) was calculated with w_2 for cases a and b, and w_1 for case c, respectively, and has been artificially smoothed with a 60 day running mean unweighted smoother (12 model output time steps).

ACPD
2, 1261–1286, 2002

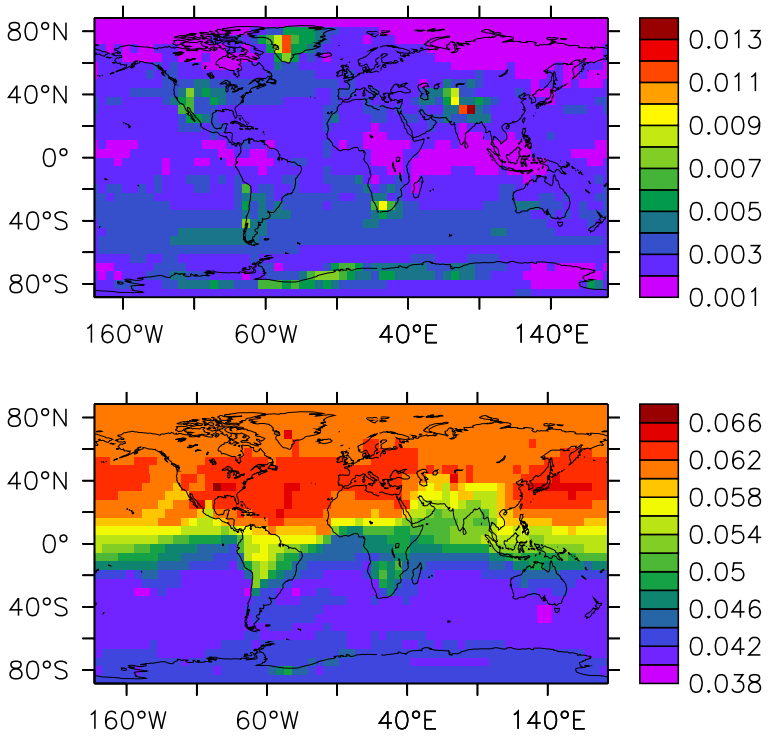

Fig. 3. Relative tracer variability (standard deviation divided by average, σ_μ/μ) for the year 1996. The upper panel shows the annual average of the 5-day variability, the lower panel the 1 year variability.

ACPD
2, 1261–1286, 2002

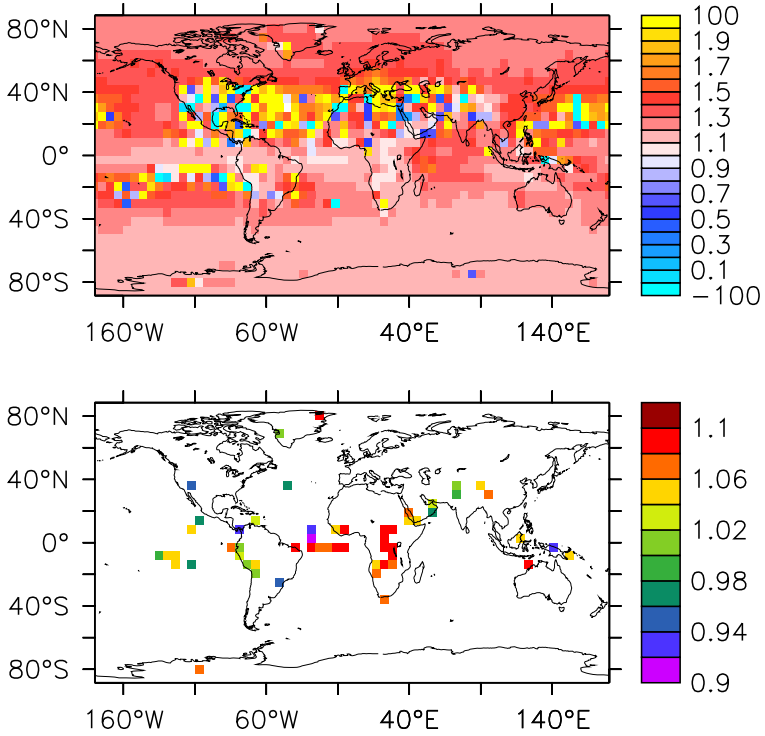

Fig. 4. Three-year average (1995–1997) ratio of local lifetime (surface), derived from the tracer rate at a given location ($\tau_s = -\mu_s/(d\mu_s/dt)$) to global average tracer lifetime ($\tau = -M/(dM/dt)$) derived from global tracer mass (Eq. (1), left). The upper panel shows the full range, the lower panel only those locations where the ratio is in the 10% range around unity. The local tracer mass mixing ratio time series have been smoothed with a 60 day running mean unweighted smoother (12 model output time steps).

ACPD
2, 1261–1286, 2002

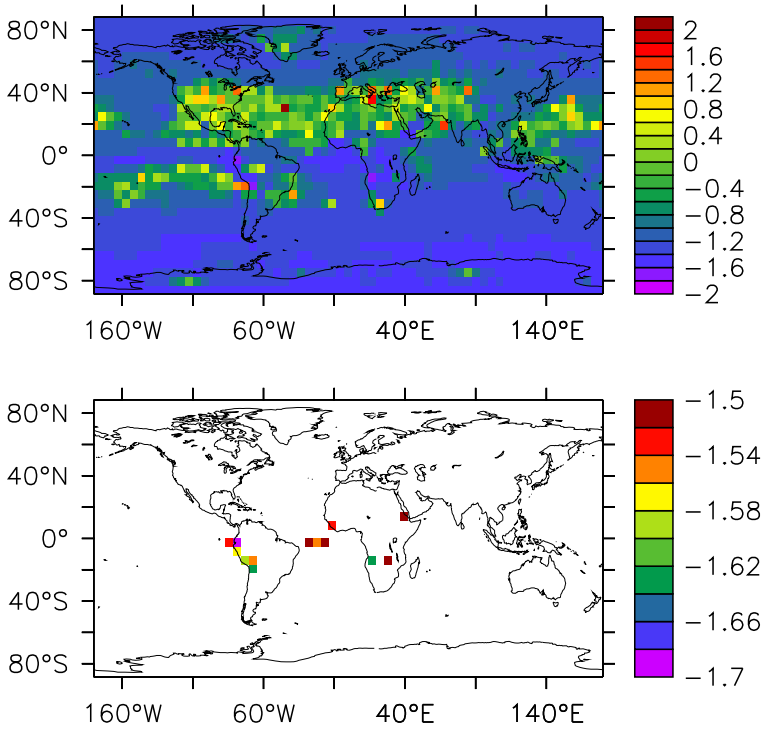

Fig. 5. Decadal logarithm of three-year average (1995–1997) RMS-deviation between local lifetime (surface), derived from the tracer rate at a given location ($\tau_s = -\mu_s/(d\mu_s/dt)$) from global average tracer lifetime derived from global tracer mass (Eq. (1), left). The upper panel shows the full range, the lower panel only those locations which are in the lower 5% of the full range. The local tracer mass mixing ratio time series have been smoothed with a 60 day running mean unweighted smoother (12 model output time steps).

ACPD
2, 1261–1286, 2002